NASA Technical Memorandum 87133

The Mechanism of Erosion of Metallic Materials Under Cavitation Attack

D.C.S. Rao
Case Western Reserve University
Cleveland, Ohio

and

D.H. Buckley
Lewis Researh Center
Cleveland, Ohio

Prepared for the
International Symposium on Cavitation
sponsored by JSME/ASME/IME(UK)/JSCE/IAHR
Sendai, Japan, April 16-19, 1986

NASA

THE MECHANISM OF EROSION OF METALLIC MATERIALS UNDER CAVITATION ATTACK

D.H. Buckley
National Aeronautics and Space Administration
Lewis Research Center
Cleveland, Ohio 44135

and

B.C.S. Rao
Case Western Reserve University
Cleveland, Ohio

SUMMARY

The mean depth of penetration rates (MDPRs) of eight polycrystalline metallic materials, Al 6061-T6, Cu, brass, phosphor bronze, Ni, Fe, Mo, and Ti-5Al-2.5Sn exposed to cavitation attack in a viscous mineral oil with a 20 kHz ultrasonic oscillator vibrating at 50 μm amplitude are reported. The titanium alloy followed by molybdenum have large incubation periods and small MDPRs. The incubation periods correlate linearly with the inverse of hardness and the average MDPRs correlate linearly with the inverse of tensile strength of materials. The linear relationships yield better statistical parameters than geometric and exponential relationships. The surface roughness and the ratio of pit depth to pit width (h/a) increase with the duration of cavitation attack. The ratio h/a varies from 0.1 to 0.8 for different materials. Recent investigations (ref. 20) using scanning electron microscopy to study deformation and pit formation features are briefly reviewed. Investigations with single crystals indicate that the geometry of pits and erosion are dependent on their orientation.

E-2684

INTRODUCTION

The erosion or damage of materials because of cavitation attack is one of the important undesirable effects associated with the occurrence of cavitation in an engineering component. Pumps, turbines, gates, valves, ships' propellers, bearings, seals, gears and many other engineering devices/components are known to suffer from this phenomenon. The situation may involve a thin layer of liquid, as in lubrication between two surfaces, or a large quantity of flowing liquid, as in flow past a valve or through a turbine. The mechanics of cavitation attack and material removal are the same in all such situations. There had been an impressive collection of data on various aspects of cavitation over the past three or four decades. However, a reasonable prediction of the occurrence of cavitation or the erosion on a given material in a given situation is still not possible.

---

*Case Western Reserve University, Cleveland, Ohio.

Cavitation attack on a surface involves repetitive impact of thin microjets or shockwaves on it. It is generally agreed that during the asymmetrical collapse of cavitation bubbles, thin microjets of high velocity are generated. Recent studies on the collapse of spark-generated bubbles by Benjamin and Ellis (ref. 1), Ellis and Starrett (ref. 2), Lauterborn and Bolle (ref. 3) and Shima et al. (ref. 4) have clearly indicated the formation of microjets in cavity collapse. The maximum diameter of cavitation bubbles formed in water is generally of the order of 2 to 4 mm, and the diameter of microjets generated is 10 to 40 μm (refs. 5,6). Kling and Hammitt (ref. 7) reported that the diameter of microjet is one-fiftieth of the initial diameter of cavitation bubble. Preece and Brunton (ref. 6) estimated the diameter of microjet to be one-tenth of the diameter of bubble. Brunton (ref. 8) estimated the velocity of microjets to be 1000 m/s.

The life of a cavitation bubble is of the order of several microseconds and the duration of microjet impact on the surface is of the order of a few nanoseconds (refs. 6,8). Vyas and Preece (refs. 9,10) measured a maximum stress amplitude of about 700 MPa (approximately 7×10^3 atm) during cavity collapse. Most of the metallic materials on which cavitation erosion was observed are polycrystalline with average grain diameters in the range of 10 to 100 μm. These details indicate that cavitation and the mechanism of resulting erosion of materials are transient microphenomena. These features have imposed limitations on the precise understanding of the phenomenon.

Because of the complex nature of cavitation erosion, several theories based on speculations were proposed. It is now generally agreed that erosion results from the mechanical action of cavitation on the surface although additional electrochemical action might accelerate the same. Most of the investigations reported on cavitation erosion concerned about gross features like mass loss, mass loss rate and correlation of erosion resistance with known mechanical properties (ref. 11). Thiruvengadum (ref. 12) suggested that strain energy of materials was responsible for their erosion resistance. Hobbs (ref. 13), Hammitt and Garcia (ref. 14), and Rao et al. (refs. 15,16) have found good correlation of erosion resistance with ultimate resilience. However, the excellent cavitation erosion resistance of materials like titanium, cobalt and their alloys could not be explained. The justification given for choosing ultimate resilience for correlating cavitation erosion resistance was that fracture occurred during cavitation erosion after elastic deformation only. It was suggested that the extremely short durations of attack did not allow the materials to go through plastic deformation. This proposition cannot, however, be justified either from theory or from experiments. Some recent investigations by Preece et al. (ref. 17), Heathcock et al. (ref. 18), Anthony and Silence (ref. 19) and Rao and Buckley (ref. 20) have focussed on properties like microstructure, crystal structure, grain size, etc. of the materials.

This paper presents recent investigations carried out to study the deformation and erosion characteristics of poly- and mono-crystalline materials exposed to cavitation attack. Variations of mean depth of penetration, its rate and surface roughness are studied. Correlations of incubation periods and erosion rates of polycrystalline materials with their mechanical properties are reported. The characteristics of deformation, pit formation and material removal are studied using optical and scanning electron microscopy. Based on these observations, the mechanism of erosion of materials is discussed.

NOMENCLATURE

a	pit radius
H	Brinell hardness
h	pit depth
IP	incubation period
MDPR	mean depth of penetration rate
n_1, n_2, n_3	exponents
PFR	pit formation rate
UR	ultimate resilience
V	peripheral velocity
WLR_{max}	maximum weight loss rate
r	radius of sphere
σ	cavitation number

EXPERIMENTAL EQUIPMENT, TEST MATERIALS, AND TEST PROCEDURES

Experimental Equipment

The experiments are carried out in an ultrasonic oscillator operating at 20 kHz frequency and a peak-to-peak amplitude of 50 μm. The amplitude of the tip of the horn could be varied from 25 to 105 μm.

Test Materials

The test specimens of polycrystalline materials are prepared from 12.7 mm diameter rods. Five metals with face-centered-cubic (fcc) matrices, viz Al 6061-T6, copper (ETP), free cutting brass, phosphor bronze and nickel; two metals with body-centered-cubic matrices, viz iron and molybdenum; and a titanium alloy Ti-5Al-2.5Sn with a hexagonal-close-packed (hcp) matrix are examined in the study. The chemical composition, density and average grain size of the materials are given in table I. The experiments are carried out in a mineral oil whose physical properties are given in table II. To examine the role of viscosity in cavitation, a thick (high viscosity) mineral oil is selected for the investigation.

Two single crystals of α-brass with 99 wt % Cu-1 wt % Zn composition and having face-centered-cubic structure are also examined. For one crystal, the face exposed to cavitation is (001) plane while for the second crystal, the face exposed to cavitation is (110) plane.

Test Procedures

The test specimen surfaces are polished using a series of emery papers down to grit 600. They are then polished using alumina powders of 1.0, 0.3 and 0.05 μm sizes over a polishing wheel.

The test specimens of polycrystalline materials are mounted at the tip of the horn, while the single crystal specimens are placed below the tip of horn at a distance of 2 mm from it. The specimen surfaces are exposed to cavitation action for the desired length of time and their weight loss, changes in roughness and details of pit formation are studied.

EXPERIMENTAL INVESTIGATIONS AND CORRELATIONS

Mean Depth of Penetration Rate

The erosion of materials is expressed as the mean depth of penetration, MDP from the surface. The MDP is computed from the weight loss measurements, the surface area and density. The mean depth of penetration rate MDPR is the average rate of erosion during a given interval. The variations of MDPR of the different polycrystalline materials are shown in figure 1. The average MDPR of Al 6061-T6, brass and copper are 99.6, 107 and 542 μm/hr respectively. The average MDPR of iron, bronze and nickel are 39.2, 26.4 and 56.1 μm/hr. Similarly, the average MDPR of titanium and molybdenum are 0.5 and 1.8 μm/hr. It may be seen that the average MDPR of the different materials varies over three orders of magnitude. The titanium alloy has the lowest average MDPR while copper has the highest. The MDP on titanium after 1800 min (30 hr) exposure to cavitation attack was only 15 μm while on copper it was 163 μm after an exposure of just 18 min.

Incubation Periods

Incubation period is an important parameter because it gives us an idea about the duration in which a material or component is not excessively damaged. As seen clearly in the case of titanium, very insignificant weight loss takes place during this period. Incubation period is defined in two different ways: (1) the duration of test for obtaining a defined value of MDP (e.g., 2 or 5 μm), and (2) the intercept on the time axis as the linear part of the erosion curve is extended to it. In the present investigation, the incubation period is taken as the duration for a MDP of 5 μm (ref. 21). The incubation periods thus obtained are given in Table III. It may be seen that molybdenum and titanium alloy have very high incubation periods.

Correlations with Mechanical Properties

As already pointed out in the introduction, many investigators have attempted to determine the property or properties of the materials responsible for erosion resistance. Such attempts have not been totally successful when a large spectrum of materials are considered and have indicated the need to understand the mechanism of erosion during cavitation attack. The present erosion data in a viscous mineral oil is correlated with the properties - hardness, yield strength, tensile strength and ultimate resilience, table III

using a least-squares technique. The correlations are made using linear, exponential and geometric relationships. Table IV presents the statistical parameters for the different correlations with incubation periods. It may be seen that hardness exhibits the best correlation followed by tensile strength, yield strength and ultimate resilience. It may also be seen that a linear relationship is better than the other two relationships. Investigations of Talks and Morton (ref. 22) showed that incubation times from open beaker tests correlate very well with rates of increase of roughness in simulated valve tests. However, they caution that incubation times do not always correlate well with erosion rates.

The correlation of inverse of MDPR with mechanical properties gives us the best property governing erosion of MDPR. In this case, tensile strength followed by ultimate resilience yields better statistical parameters than other properties. Also, a linear relationship is once again better than the others. From experiments with four different steels, a brass and aluminum, Talks and Morton (ref. 22) found an asymptotic relationship between material hardness and cavitation erosion resistance. For hardness Hv 400, the erosion resistance of materials did not increase. Okada et al. (ref. 23) found good correlation between erosion resistance and ultimate resilience for cavitation erosion data of four sintered carbon materials used for mechanical face seals.

Zhiye (ref. 24) investigated cavitation erosion of three alloys, viz babbitt metal, common brass and propeller brass, and rubber in a rotating disk apparatus. He found that the pit formation rate PFR varied with peripheral velocity V and ultimate resilience UR of the materials as:

$$PFR \propto V^{n_1} \tag{1}$$

where

$$n_1 \simeq 0.1/UR \tag{2}$$

He also found that maximum weight loss rate WLR_{max} varied with the Brinell hardness H of the materials according to the equation:

$$1/WLR_{max} \propto H^{n_2} \tag{3}$$

where

$$n_2 \simeq 0.51/\sigma \tag{4}$$

in which σ = cavitation number. Zhou and Hammitt (ref. 25) suggest the following exponential type of relationship between MDPR and incubation period IP:

$$(MDPR)^{-1} \propto (IP)^{n_3} \tag{5}$$

They obtained values of $n_3 = 0.93$ for their vibratory erosion data and $n_3 = 0.95$ for their venturi data.

Surface Roughness and Geometry of Pits

Surface roughness measurements (ref. 20) taken at different intervals show increased roughness with cavitation attack. The depth of pits increased faster than their width. A cavitation pit is generally assumed to be a segment of a sphere. If 2a is the pit diameter and h is the pit depth, the radius r of the sphere can be expressed as:

$$r = \frac{a^2 + h^2}{2h} \tag{6}$$

$$h/a = \left(\frac{2r}{h} - 1\right)^{-1/2} \tag{7}$$

Figure 2 presents a plot of h/a against (2r/h) - 1 for the different materials. The values of h/a vary from 0.10 to 0.8 and in general increase with cavitation attack. It is not clear at this time whether the range of those values is controlled by parameters like grain size, strength properties, crystal structure, etc. Previous measurements of pit size for cavitation erosion in water by Robinson and Hammitt (ref. 26) indicated the ratio h/a to be 0.20. Stinebring et al. (ref. 27) determined the minimum and maximum values of h/a to be 0.068 and 0.332 respectively in their experiments in water.

Scanning Electron Microscopy

To understand the mechanism of deformation and formation of pits during cavitation attack, scanning electron microscopic observations are carried out at different intervals. Figures 3(a) to (c) present three typical micrographs of polycrystalline brass. After a cavitation attack for 10 s, figure 3(a) tiny pits are observed over grain boundaries. The grain boundary voids and softer lead precipitates appear to be favorable spots for early pit formation (ref. 20). With continued cavitation attack, the pits at the junction of three or more grain boundaries, figure 3(b) grow by erosion of the adjoining grains. During the early cavitation attack, considerable plastic deformation of grains through slip and twinning is noticed (ref. 20). Figure 3(c) shows a typical pit formation over a grain surface. The pits on grain surfaces appear to be dependent on the orientation of the individual grains. This aspect is clearly seen in the micrographs of pits on single crystals presented in the next paragraph.

Figures 4(a) and (b) present two micrographs of pits on α-brass single crystals of two orientations. The pits on crystal with (001) face exposed to cavitation are squares with rounded edges, figure 4(a) while the pits on crystal with (110) face exposed to cavitation are elongated in 110 direction, figure 4(b). Measurements of the variations of weight loss with test time of the two single crystals exposed to cavitation attack showed that crystal B with (110) face exposed to cavitation erodes faster than crystal A with (001) face exposed to cavitation. Measurements of surface roughness also showed that the pits in the case of crystal B are deeper and more closely spaced than those on crystal A.

Based on the investigations presented in the preceding sections, the mechanism of cavitation erosion of polycrystalline metallic materials could be visualized as follows. Cavitation attack involves a localized impact of repeated stress pulses over areas of the order of a few square micrometers on the surface. Early pit formation occurs on grain boundary voids, precipitates and surface defects. The pit formation and erosion of grains involves plastic deformation through slip and twinning and these features are influenced by the orientation of grains and their crystal structure in addition to other material properties. A large part of erosion occurs through a continuous process of localized plastic deformation and fracture of surface grains.

CONCLUSIONS

1. The mean depth of penetration rate, MDPR on different polycrystalline materials varied over three orders of magnitude. The titanium alloy had the lowest average MDPR of 0.5 μm/hr while copper had the highest average MDPR of 542 μm/hr.

2. The titanium alloy followed by molybdenum had the largest incubation period. The incubation periods correlate linearly with the inverse of hardness of materials. The average MDPRs correlate linearly with inverse of tensile strength followed by ultimate resilience.

3. The ratio of pit depth to pit radius varied from 0.10 to 0.8 for different materials and increased with cavitation attack.

4. Early cavitation pits formed over grain boundaries and precipitates. The pits formed at the junction of grain boundaries grew faster than the others. The pit formation over grain surfaces required longer cavitation attack than the grain boundaries.

5. The geometry of pits and erosion are dependent on the orientation of single crystals.

REFERENCES

1. Benjamin, T.B. and Ellis, A.T., "The Collapse of Cavitation Bubbles and the Pressures Thereby Produced Against Solid Boundaries," Philosophical Transactions, Series A, Vol. 260, 1966, pp. 221-240.

2. Ellis, A.T. and Starrett, J.E., "Observation on Bubble Dynamics in Jet Flow and at High Ambient Pressures," Proc. 5th Intl. Conf. on Erosion by Solid and Liquid Impact, Cambridge, England, 1979, Paper 57.

3. Lauterborn, W. and Bolle, H., "Experimental Investigation of Cavitation-Bubble Collapse in Neighborhood of a Solid Boundary," Journal of Fluid Mechanics, Vol. 72, Nov. 1975, pp. 391-399.

4. Shima, A., Takayama, K., Tomita, Y. and Oksawa, M., "Mechanisms of Impact Pressure Generation from Spark-Generated Bubble Collapse Near a Wall," AIAA Journal, Vol. 21, No. 1, January 1983, pp. 55-59.

5. Hammitt, F.G., "Cavitation and Multiphase Flow Phenomenon," McGraw Hill Book Co., Inc. 1980.

6. Preece, C.M. and Brunton, J.H., "A Comparison of Liquid Impact Erosion and Cavitation Erosion," Wear, Vol. 60, 1980, pp. 269-281.

7. Kling, C.L. and Hammitt, F.G., "A Photographic Study of Spark-Induced Cavitation Bubble Collapse," Journal of Basic Engineering, Trans. ASME, Vol. 94, Series D, No. 4, December 1972, pp. 825-833.

8. Brunton, J.H., "Cavitation Damage," Proc. 3rd Intl. Congress on Rain Erosion, August 1970.

9. Vyas, B. and Preece, C.M., "Cavitation Erosion of Face-Centered-Cubic Metals," Metallurgical Transactions, Vol. 8A, June 1977, pp. 915-923.

10. Vyas, B. and Preece, C.M., "Stress Produced in a Solid by Cavitation," Journal of Applied Physics, Vol. 47, No. 12, December 1976, pp. 5133-5138.

11. Knapp, R.T., Daily, J.W., and Hammitt, F.G., "Cavitation," McGraw Hill Book Co. Inc., New York, 1970, pp. 321-443.

12. Thiruvengadam, A., "A Unified Theory of Cavitation Damage," Journal of Basic Engineering, Trans. ASME, Vol. 85, No. 3, Sept. 1963, pp. 365-376.

13. Hobbs, J.M., "Experience with a 20 kc Cavitation Erosion Test," ASTM Spec. Tech. Publ. 408, 1967, pp. 159-179.

14. Garcia, R. and Hammitt, F.G., "Cavitation Damage and Correlations with Material and Fluid Properties," Journal of Basic Engineering, Trans, ASME, Vol. 89, No. 4, December 1967, pp. 753-763.

15. Rao, B.C.S., Rao, N.S.L. and Seetharamiah, K., "Cavitation Erosion Studies with Venturi and Rotating Disk in Waters," Journal of Basic Engineering, Trans. ASME, Vol. 92, No. 3, Sept. 1970, pp. 563-579.

16. Rao, B.C.S., Rao, P.V. and Rao, N.S.L., "Evaluation of Erosion Resistance of Metallic Materials and the Role of Material Properties in Correlations," Journal of Testing and Evaluation, Vol. 7, No. 3, May 1979, pp. 133-146.

17. Preece, C.M., Vaidya, S. and Dakshinamurthy, S., "Influence of Crystal Structure on the Failure Mode of Metals by Cavitation Erosion," in W.F. Adler (ed), Erosion: Prevention and Useful Applications, ASTM STP 64, 1979, pp. 409-433.

18. Heathcock, C.J., Protheroe, B.E. and Ball, A. in P. Hasen, V. Gerold, and G. Kostotz (eds), Proc. 5th Intl. Conf. on Strength of Metals and Alloys, Aachen, August, 1979, Vol. 1, Pergamon, Oxford, 1979, pp. 219-224.

19. Anthony, K.C. and Silence, W.L., "The Effect of Composition and Microstructure on Cavitation Erosion Resistance," Proc. 5th Intl. Conf. on Erosion by Solid and Liquid Impact, Cambridge, England, 1983, paper 67.

20. Rao, C.C.S. and Buckley, D.H., "Deformation and Erosion of FCC Metals and Alloys Under Cavitation Attack," Materials Science and Engineering, Vol. 67, No. 1, 1984, pp. 55-67.

21. Talks, M.G. and Morton, G., "Cavitation Erosion of Fire-Resistant Hydraulic Fluids," Proc. ASME Fluids Engineering Conference, Boulder, Colorado, June 1981, pp. 139-152.

22. Okada, T., Wai, Y. and Hosakawa, Y., "Comparison of Surface Damage Caused by Sliding Wear and Cavitation Erosion on Mechanical Face Seals," ASME/ASLE Joint Lubrication Conference, San Diego, California, October 1984.

23. Zhiye, Ji, "Experimental Investigation on Cavitation Erosion with Rotating Disk," Proc. ASME Cavitation Conference, Albuquerque, New Mexico, June 1985, pp. 31-39.

24. Zhou, Y.K. and Hammitt, F.G., "Recent Results from Cavitation Tests at the University of Michigan," Proc. ASME Cavitation Conference, Albuquerque, New Mexico, June 1985, pp. 77-85.

25. Robinson, M.J. and Hammitt, F.G., "Detailed Damage Characteristics in a Cavitating Venturi," Journal of Basic Engineering, Trans. ASME, Vol. 89, 1967, pp. 161-173.

26. Stinebring, D.R., Holl, J.W. and Arndt, R.E.A., "Two Aspects of Cavitation Damage in the Incubation Zone: Scaling by Energy Consideration and Leading Edge Damage," Journal of Fluids Engineering, Trans. ASME, Vol. 102, 1980, pp. 481-485.

TABLE I. - CHEMICAL COMPOSITION, CRYSTAL STRUCTURE, DENSITY AND AVERAGE GRAIN SIZE OF THE METALS

Material	Chemical composition, wt %	Crystal structure	Density, g/cm^3	Measured average grain size, μm
Al 6061-T6	Al-1.0Mg-0.6Si-0.25 Cu-0.25Cr	fcc	2.70	20
Cu (ETP)	99.95Cu-0.04o	↓	8.89	75
Brass	Cu-35.5Zn-3Pb	↓	8.50	10
Phosphor bronze	Cu-2.6Sn-0.6P-3Pb-0.07Zn	↓	8.86	35
Nickel	99.9 percent Ni	↓	8.90	(a)
Iron	99.9 percent Fe	bcc	7.87	25
Molybdenum	99.9 percent Mo	bcc	10.22	(a)
Titanium	Ti-5Al-2.5Sn	hcp	4.48	15

[a]Not measured.

TABLE II. - PHYSICAL PROPERTIES OF MINERAL OIL[a]

Property	
Density, kg/m^3	869
Kinematic viscosity at 20 °C, cs	110
Surface tension at 20 °C, dyn/cm	33.2
Bulk modulus, GPa	1.7
Flash point, °C	213
Pour point, °C	-9.4

[a]Drakeol 21 furnished by Penreco.

TABLE III. - MECHANICAL PROPERTIES OF THE MATERIALS AND INCUBATION PERIODS

Ref. T. Lyman (ed) Metals Handbook, vol. 1, American Society of Metals, Metals Park, OH, 1967.

Material	Hardness, DPH	Yield strength, MPa	Tensile strength, MPa	Ultimate resilience, MPa	Elastic modulus, GPa	Incubation[a] period, min
Al 6061-T6	107	276	310	0.707	68	1.3
Cu (ETP)	90	69	220	.210	115	0.67
Brass	90	125	340	.596	97	6.2
Phosphor Bronze	150	448	517	1.215	110	16.5
Nickel	64	59	317	.242	207	10.2
Iron	63	50	276	.183	208	14
Molybdenum	300	300	450	.326	310	270
Ti-5Al-2.5Sn	355	807	862	3.377	110	600

[a]Measured.

TABLE IV. - CORRELATION OF INCUBATION PERIODS WITH MATERIAL PROPERTIES

Material property	Type of correlation	CD	CC	SE	A	B
Hardness	L	0.87	0.93	0.14	-0.26	1.06
	E	.73	.85	1.33	1.62	6.32
	G	.60	.77	1.60	.44	2.76
	L	.80	.90	.17	-.46	1.36
Tensile strength	G	.71	.84	1.36	1.12	4.63
	E	.66	.81	1.43	.01	8.00
	L	.70	.84	.21	-.12	.93
Yield strength	E	.47	.68	1.85	.01	4.96
	G	.34	.58	2.06	.19	1.33
	L	.69	.83	.22	-.05	.94
Ultimate resilience	E	.37	.61	2.02	7.85	4.46
	G	.23	.4	2.22	.20	1.13

CD - Coefficient of Determination
CC - Coefficient of Correlation
SE - Standard Error of Estimate
L - Linear $Y = A + BX$
E - Exponential $Y = A \text{ Exp } BX$
G - Geometric $Y = AX$

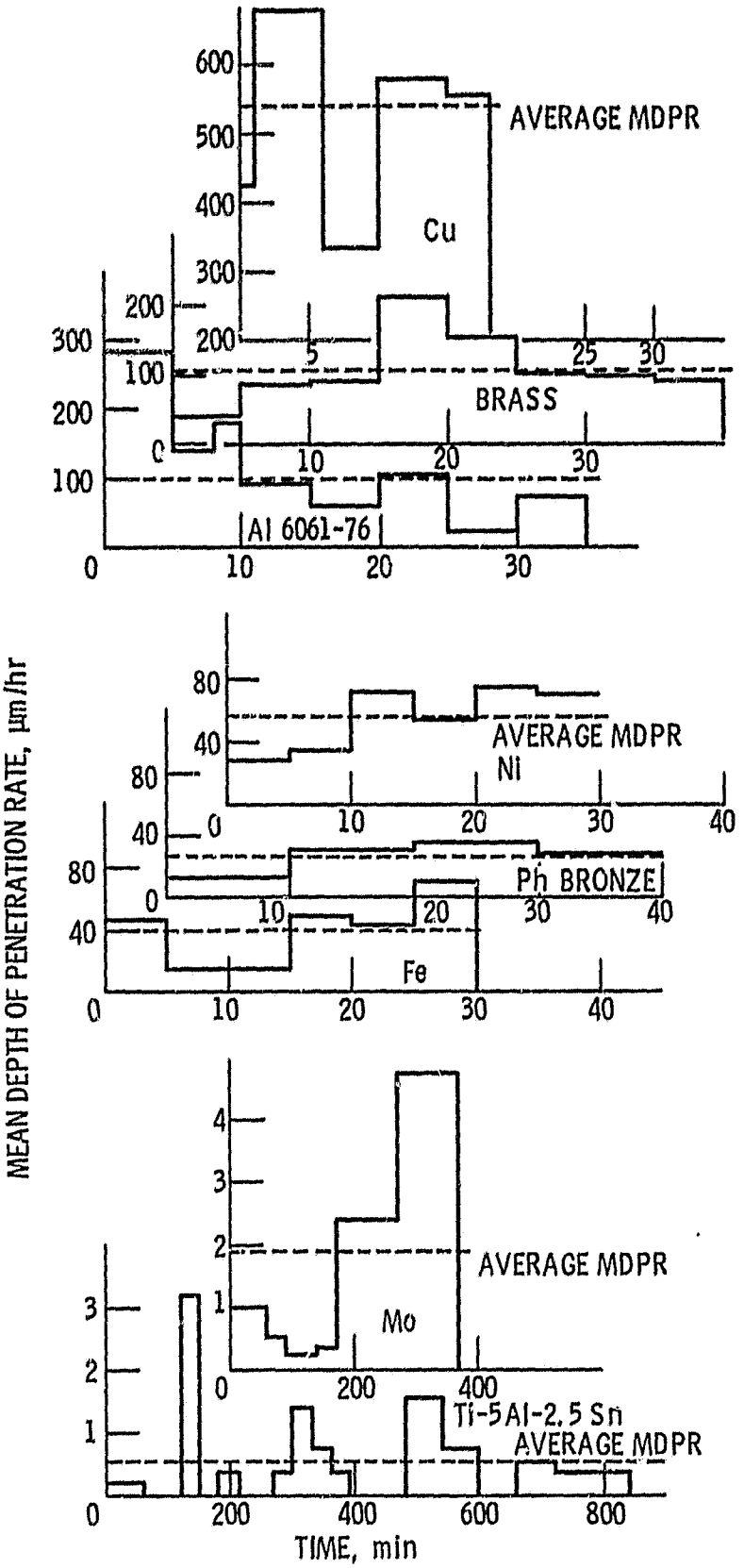

Figure 1. - Variations of MDPR with time.

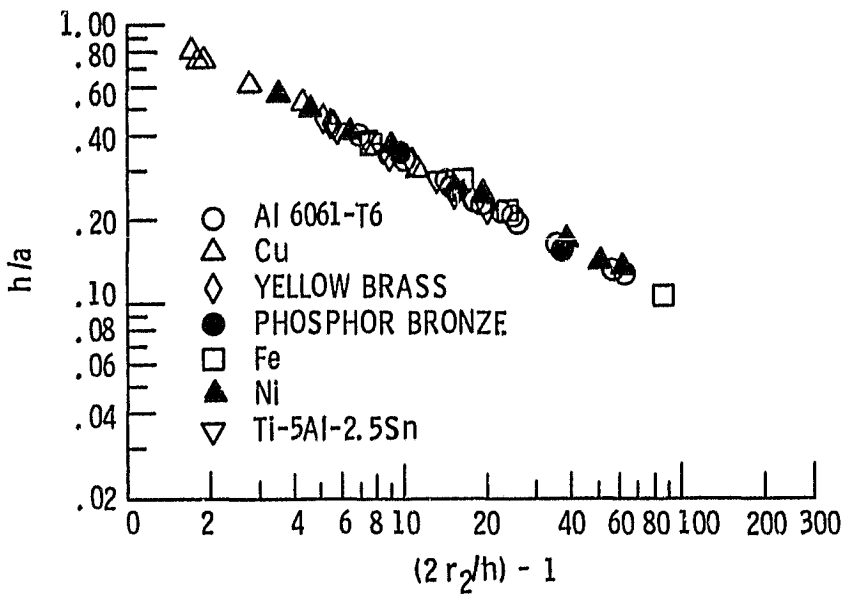

Figure 2. - Variation of the ratio h/a with $(2r_2/h) - 1$.

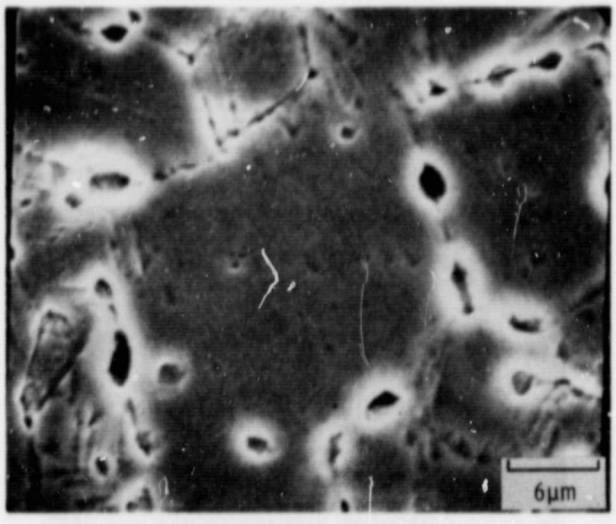

(a) t = 10 s, showing grain boundary attack.

(b) t = 50 s, showing growth of pits at the junction of grain boundaries.

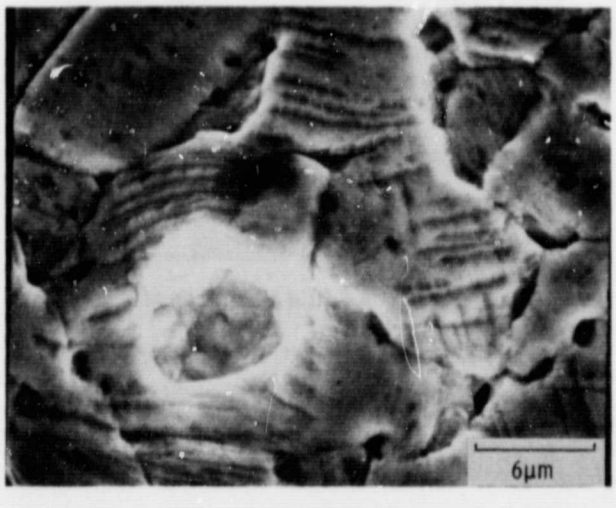

(c) t = 50 s, showing pit formation over a grain surface.

Figure 3. - Scanning electron micrographs of cavitation attack on brass surface.

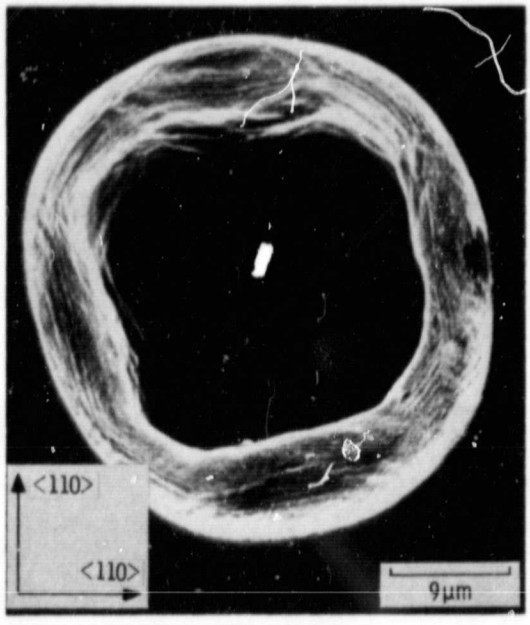

(a) t=15 min, A typical pit on (001) face.

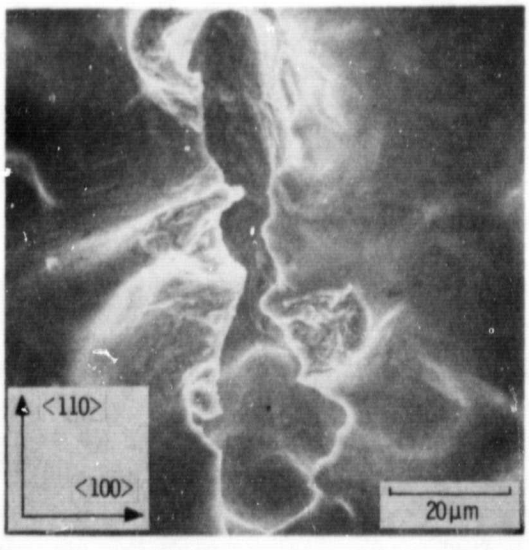

(b) t=90 min, A typical pit on (110) face.

Figure 4. - Scanning electron micrographs of cavitation attack on α-brass single crystals.

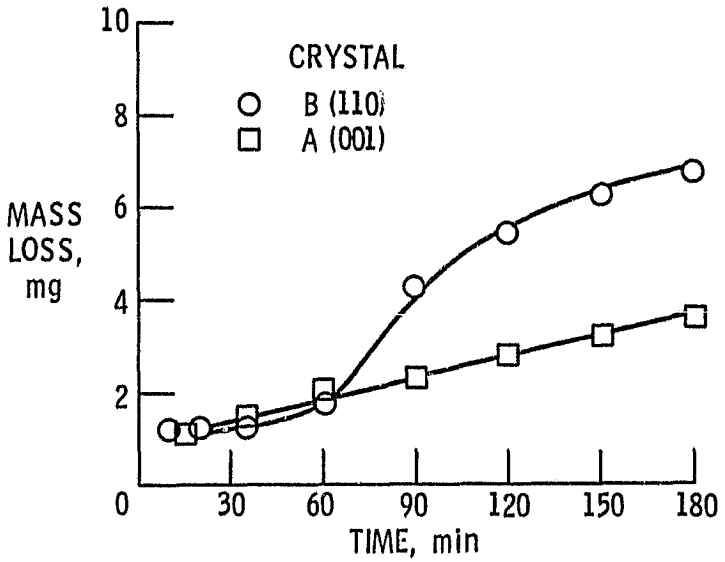

Figure 5. - Variation of weight loss with time-single crystals.

1. Report No.	2. Government Accession No.	3. Recipient's Catalog No.
NASA TM-87133		

4. Title and Subtitle	5. Report Date
The Mechanism of Erosion of Metallic Materials Under Cavitation Attack	6. Performing Organization Code: 506-53-1B

7. Author(s)	8. Performing Organization Report No.
B.C.S. Rao, Case Western Reserve University, Cleveland, Ohio, and D.H. Buckley, Lewis Research Center	E-2684
	10. Work Unit No.

9. Performing Organization Name and Address	11. Contract or Grant No.
National Aeronautics and Space Administration Lewis Research Center Cleveland, Ohio 44135	13. Type of Report and Period Covered: Technical Memorandum

12. Sponsoring Agency Name and Address	14. Sponsoring Agency Code
National Aeronautics and Space Administration Washington, D.C. 20546	

15. Supplementary Notes

Prepared for the International Symposium on Cavitation sponsored by JSME/ASME/IME(UK)/JSCE/IAHR, Sendai, Japan, April 16-19, 1986.

16. Abstract

The mean depth of penetration rates (MDPRs) of eight polycrystalline metallic materials, Al 6061-T6, Cu, brass, phosphor bronze, Ni, Fe, Mo, and Ti-5Al-2.5Sn exposed to cavitation attack in a viscous mineral oil with a 20 kHz ultrasonic oscillator vibrating at 50 μm amplitude are reported. The titanium alloy followed by molybdenum have large incubation periods and small MDPRs. The incubation periods correlate linearly with the inverse of hardness and the average MDPRs correlate linearly with the inverse of tensile strength of materials. The linear relationships yield better statistical parameters than geometric and exponential relationships. The surface roughness and the ratio of pit depth to pit width (h/a) increase with the duration of cavitation attack. The ratio h/a varies from 0.1 to 0.8 for different materials. Recent investigations (20) using scanning electron microscopy to study deformation and pit formation features are briefly reviewed. Investigations with single crystals indicate that the geometry of pits and erosion are dependent on their orientation.

17. Key Words (Suggested by Author(s))	18. Distribution Statement
Erosion; Cavitation; Polycrystalline materials; Single crystals; Mineral oil	Unclassified - unlimited STAR Category 37

19. Security Classif. (of this report)	20. Security Classif. (of this page)	21. No. of pages	22. Price*
Unclassified	Unclassified		

*For sale by the National Technical Information Service, Springfield, Virginia 22161